Hindawi
Advances in Civil Engineering
Volume 2021, Article ID 3427451, 7 pages
https://doi.org/10.1155/2021/3427451

Research Article

Effect of Low Temperatures on the Mechanical Performance of GFRC Modified by Low Carbon Cement

Meimei Song[1] **and Chuanlin Wang**[2]

[1]*Department of Mechanical Engineering, Xi'an Shiyou University, Xi'an, China*
[2]*College of Engineering, Shantou University, Shantou, China*

Correspondence should be addressed to Chuanlin Wang; clwang@stu.edu.cn

Received 14 July 2021; Revised 27 September 2021; Accepted 28 September 2021; Published 8 October 2021

Academic Editor: Xianming Shi

Glass fibre reinforced cement (GFRC) is a composite material with great ductility but it undergoes severe strength and ductility degradation with ageing. Calcium sulfoaluminate (CSA) cement is low carbon cement, and more importantly, it exhibits great potential to produce more ductile and durable GFRC. This study focuses on mechanical performance, e.g., compressive strength, stress-strain curve, and freeze-thaw resistance of CSA/GFRC as well as its microstructural characteristics under low temperatures. XRD was applied to investigate the hydration mechanism of CSA cement under −5°C, 0°C, and 5°C. It was found out that low-temperature environments have very little effect on the type of hydration products, and the main hydration product of hydrated CSA cement cured under low temperatures is ettringite. Moreover, low-curing temperatures have an adverse effect on the compressive strength developments of CSA/GFRC but the strength difference compared with that under 20°C reduces gradually with increasing curing ages. In terms of bending performance, both ultimate tensile strength and ultimate strain value indicate considerable degradation with ageing under low temperatures after 14 d. The ultimate strain value reduces to 0.34% at −5°C, 0.39% at 0°C, and 0.44% at 5°C compared with 0.51% for that cured at 20°C for 28 d. The tensile strength of samples cured at −5°C for 28 d is only 15.2 MPa, taking up only 40% of that under 20°C. CSA/GFRC also demonstrated great capability in the antifreeze-thaw performance, and the corresponding strength remains 95.9%, 94.7%, 94.2%, and 94.3%, respectively, for that cured under 20°C, 5°C, 0°C, and −5°C after 50 freeze-thaw cycles. Microstructural studies reveal that densification of the interfilamentary space with intermixtures of C-A-S-H and ettringite is the main reason that causes the degradation of CSA/GFRC, which may result in loss on flexibility when forces are applied, therefore reducing the post-peak toughness to some extent.

1. Introduction

Glass fibre reinforced cement (GFRC) is widely applied in practical engineering, e.g., façade panel and pavement over the past two decades; this can be attributed to its superior ductility resulted from the bridging effect of glass fibre [1–3]. However, it was reported that severe reductions in compressive strength and ductility may occur in GFRC with ageing [4, 5], which has become a common concern for the service life of engineering members made of GFRC. The intrinsic microstructural reasons corresponding to this degradation are normally associated with chemical corrosion of fibre by the alkalinity in pore solution [6] and severe CH densification between and around fibres that results in loss of flexibility [7]. At the same time, in the global background of low carbon emission, cement industry is faced with great challenge as it contributed about 6% to total global anthropogenic CO_2 emission every year [8, 9]. Therefore, in order to produce more environmental friendly, ductile, and durable GFRC, efforts should be made to study the modified cement matrix with lower carbon emission, lower CH formation, and reduced alkalinity in the pore solution.

Calcium sulfoaluminate (CSA) cement is characterized as a kind of low carbon cementitious material due to lower calcium content in the raw materials and a lower burning temperature at 1250°C, which is about 200°C lower than that for the production of Portland cement. More importantly,

CSA cement has superior antifreeze property, high compressive strength, and durability [10–12]. In addition, extremely low alkalinity can also be discovered in the pore solution of CSA cement due to the absence of CH during hydration process [13], which can provide a less aggressive environment for the durability of embedded glass fibre. Therefore, CSA cement possesses great potential to produce more environmental friendly, ductile, and durable GFRC.

GFRC modified by CSA cement (CSA/GFRC) has aroused great attention among researchers, and many studies have been undertaken to investigate its mechanical properties and microstructural characteristics under different curing regimes [14–16]. Research by Peʃra and Ambroise [17] showed that CSA/GFRC exhibited rapid development of modulus of rupture, which reaches 8 MPa at 3 h, 9.3 MPa at 24 h, and 20.5 MPa at 28 d. Song et al. [15] demonstrated that CSA/GFRC still retained a large proportion of toughness after ageing for 10 years at 25°C. There were insignificant changes in the composite strength compared with the unaged sample, and the fibres still showed great ability to absorb energy and may control crack growth by bridging effect. Corresponding ultimate strain reduced to about 0.5% compared with a value of 0.8% for the unaged sample. Microstructural studies revealed that the space between and around the glass fibres was considerably vacant and porous. Research by Purnell and Beddows [5] reported that under accelerated ageing at 50°C for 140 d, tensile strength and ultimate strain of CSA/GFRC remained almost unchanged. However, at a longer age of 316 d under the same regime, corresponding ultimate tensile strength exhibited a medium reduction from 30 MPa to 22 MPa but the bridging effect provided by glass fibres was still obvious.

In cold environments, when the hydraulic pressure caused by freezing water exceeds the tensile strength of GFRC, local cracking may initiate which significantly threatens the safety and service life of GFRC structures. More importantly, freeze-thaw cycles generated under cold environment may cause multiphase damage media of water, ice, cement, and aggregate, and the uneven frost heaving force and deformation may subsequently lead to cracking propagation. It was reported that CSA cement has favorable antifreeze property due to the high compactness within the matrix which is beneficial to resist the freezing pressure and expansion pressure to some extent [12]. Research by Li et al. [18] indicated that flexural strength of CSA cement mortar was maintained 95% after 56 cycles of freeze-thaw were conducted. Janotka and Krajei [19] demonstrated that the dynamic modulus of elasticity of CSA cement mortar was maintained 95% after 34 cycles of freeze-thaw, and crack propagation was also observed on the surface of CSA cement mortar.

In conclusion, CSA cement has favorable antifreeze property and indicates great potential to produce durable GFRC under low temperatures. However, previous studies on CSA/GFRC mainly concentrated on its mechanical properties and microstructure characteristics under standard curing or hot water accelerated ageing while the performance of CSA/GFRC under cold temperatures remains not fully understood; this is of great significance before wider application of CSA/GFRC under low temperatures can be made. The present study aims to investigate the effect of low temperatures on the hydration mechanism, stress-strain performance, and freeze-thaw cycle property of CSA/GFRC, and the underlying microstructure changes are also investigated to correlate to the changes in macroproperties.

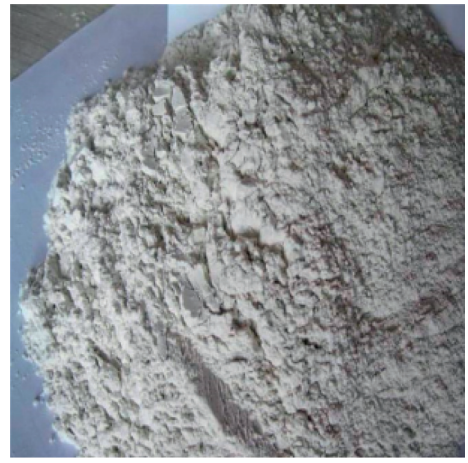

Figure 1: Commercial CSA cement used in the present study.

2. Materials and Methods

2.1. Materials. To produce CSA/GFRC, commercial CSA cement produced by Dengdian Cement Group in China was used in the present study, as shown in Figure 1. CSA cement and OPC were mixed with a ratio of 3 : 7, and quartz sand was added with a sand to cement ratio of 1 : 1. A water to cement ratio of 0.3 was applied in this study. Chemical compositions of CSA cement and ordinary Portland cement (OPC) used in this study are listed in Table 1. In order to improve the brittleness of cementitious materials, 0.5 wt. % glass fibre was added in the dry mix to produce CSA/GFRC composites. Glass fibre was chopped and randomly orientated in the form of bundles. The detailed mixing design is listed in Table 2.

2.2. Experimental Work

2.2.1. XRD Analysis. Corresponding cement pastes were prepared for XRD analysis to investigate the hydration products of CSA-based cement under low temperatures. XRD was carried out by Bruker D8 using CuKα1 radiation, and XRD data of the powder samples were collected in a 2θ range of 5° to 60° with a step size of 0.02°. After casting for 24 h, the specimens were cured in a water bath set at a temperature of 20 ± 1°C. At a curing age of 7 d, the samples were ground into fine powder and then applied in the XRD equipment for testing.

2.2.2. Mechanical Testing. CSA/GFRC was cast in two different sizes, i.e., a thin slab size (250 mm × 50 mm × 10 mm) for stress-strain performance testing and a cubic size

Table 1: Chemical compositions of CSA and OPC cement.

Composition (%)	SiO_2	Al_2O_3	Fe_2O_3	CaO	MgO	SO_3	TiO_2	Loss
CSA	8.92	32.15	1.32	44.68	1.71	8.92	1.85	0.54
OPC	19.38	4.99	1.96	63.69	2.33	4.95	0.47	2.23

Table 2: Mixing design of CSA/GFRC.

OPC (kg/m^3)	CSA (kg/m^3)	Water (kg/m^3)	Sand (kg/m^3)	Retarder (kg/m^3)	Glass fibre (wt. %)
666.7	285.7	285.7	952.4	4.8	0.5

(100 mm × 100 mm × 100 mm) for both compressive strength and antifreeze testing. After casting for 24 h, they were demolded and continued to be cured under different temperatures (−5°C, 0°C, 5°C, and 20°C) for 1, 3, 7, 14, and 28 d.

Four-point bending test was undertaken by Tinius Olsen H25KS with a major span of 200 mm and a load rate at 1.8 mm/min; relative experimental setup is shown in Figure 2. In this study, stress-strain performance of CSA/GFRC under −5°C, 0°C, 5°C, and 20°C for 1, 3, 7, 14, and 28 d was tested, respectively. In order to investigate the durability of CSA/GFRC under cold climates, antifreeze testing was also undertaken according to Chinese Standard GB/T50082-2009 (the standard for test method of long-term performance and durability of ordinary concrete). Before testing, the reference samples were still kept under the standard curing condition, but the specimens for antifreeze testing were taken out and then restored in water at 20 ± 1°C for 4 d. Then, CSA/GFRC samples were weighed and then put in the freeze-thaw testing chamber (set at −5°C, 0°C, and 5°C) for 6 h.

2.2.3. Microstructure Analysis. SEM was undertaken by JEOL JSM-5800LV equipped with EDX. Backscattered electron imaging mode was selected to characterize the morphologies on polished surfaces of CSA/GFRC. Elemental mapping was applied to investigate the arrangement of chemical elements within the matrix. In order to investigate the chemical compositions at the interfilamentary space, three representative points at the interfilamentary space were selected to give overall information on the hydrated phases between fibres.

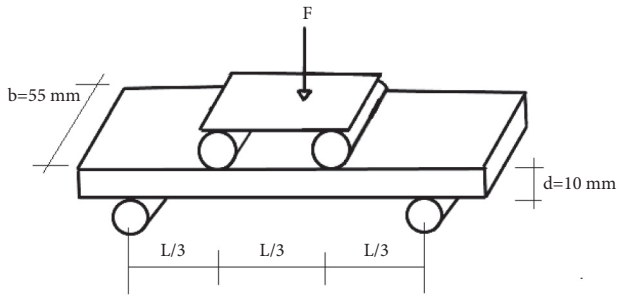

Figure 2: Experimental setup of the four-point bending test.

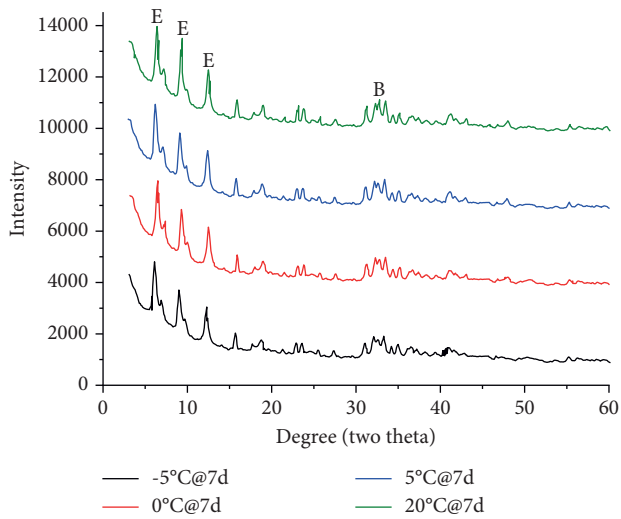

Figure 3: XRD pattern of CSA pastes cured at −5°C, 0, 5°C, and 20°C at 7 d.

3. Results and Discussion

3.1. XRD Analysis. XRD results of corresponding CSA cement pastes cured at −5, 0, 5, and 20°C for 7 d are shown in Figure 3. It can be found out that low-temperature environments have very little effect on the type of hydration products of CSA modified cement. Crystalline CH is still absent, and large amounts of ettringite can be traced in all the specimens of CSA modified cement under low-curing temperatures, which is in agreement with the previous research [14, 16]. The sharp peak of ettringite in the CSA paste cured at −5°C suggests that hydration of CSA cement still continues at lower temperature, which is beneficial for the development of both strength and densified microstructure.

It was reported that formation of ettringite was extremely sensitive to curing temperatures and decreased levels of ettringite are generated under low temperatures [12]. This is because lower curing temperature is not conducive to the breaking of chemical bond and thus may lead to a slower nucleation rate of ettringite, especially for those below 0°C [16]. In addition, a broad peak at about 32° indicates remnants of unhydrated belite clinker in all the specimens. This can be explained that hydration of calcium sulfoaluminate initiates rapidly once in contact with water, and it continues readily in the first 1-2 days; therefore, insufficient water will be remained for the hydration of belite at early ages [20]. In particular, the broad peak of belite remnants in

the CSA paste cured at −5°C suggests that hydration degree of CSA cement is limited to some extent under lower temperatures [21].

3.2. Compressive Strength. Compressive strength of CSA/GFRC cured under −5, 0, 5, and 20°C for 1 d, 3 d, 7 d, and 28 d is shown in Figure 4. It can be found out that low-curing temperatures, especially those below 0°C, have an adverse effect on the compressive strength development of CSA/GFRC. At an early age of 1 d, CSA/GFRC under lower temperatures exhibited an extremely low compressive strength compared with that cured at 20°C. The corresponding compressive strength is only 8.2 MPa, 10.5 MPa, and 16.7 MPa under −5°C, 0°C, and 5°C, which is 35.8%, 45.8%, and 72.9% of that cured at 20°C. This is because ettringite is the main contributions to the early strength of CSA cement and reduced ettringite is generated at lower curing temperatures owning to a reduced nucleation rate [12]. With increasing curing ages, CSA/GFRC obtained quick strength development under lower temperatures, and strength difference with that under 20°C is reduced gradually. In detail, compressive strength reaches 40.3 MPa, 47.2 MPa, and 50.2 MPa under −5°C, 0°C, and 5°C for 28 d, which occupies 67.7%, 79.3%, and 84.4% of that under 20°C. The relatively rapid strength development of CSA/GFRC under low-curing temperatures suggests that it can ensure the basic construction requirement in winter, and further mechanical performance needs to be investigated before wider application can be made.

3.3. Stress-Strain Performance. Stress-strain performances of CSA/GFRC cured under low temperatures for 1 d, 7 d, 14 d, and 28 d are illustrated in Figure 5. It can be observed that there is insignificant changes in the ultimate strain value at low temperatures at 1 d, which is 0.67% for −5°C, 0.78% for 0°C, and 0.87% for 5°C, respectively, compared with 0.82% for 20°C. However, low-curing temperatures have an adverse effect on the ultimate tensile strength of CSA/GFRC at early ages. It reduces to ~25 MPa at 5°C, 23 MPa at 0°C, and 18 MPa at −5°C, which is 83.3%, 76.7%, and 60.0% compared with that at 20°C.

With a progressive curing age until 14 d, CSA/GFRC demonstrates slight degradation in stress but it still exhibits great ductility properties. At a longer curing age of 28 d, there are obvious reductions in both ultimate strain value and ultimate tensile strength. For example, the ultimate strain value reduces to 0.34% at −5°C, 0.39% at 0°C, and 0.44% at 5°C compared with 0.51% for that cured at 20°C. The tensile strength of samples cured at −5°C for 28 d is only 15.2 MPa, taking up only 40% of that under 20°C.

It can be concluded that there is less influence of low-curing temperatures on the ductility properties of CSA/GFRC at early ages; however, both ultimate tensile strength and ultimate strain value indicate medium degradation after 14 d. This degradation process is similar to the previous results on CSA/GFRC [5, 16], in which CSA/GFRC indicates gradual and medium reduction on both strength and ductility under accelerated ageing.

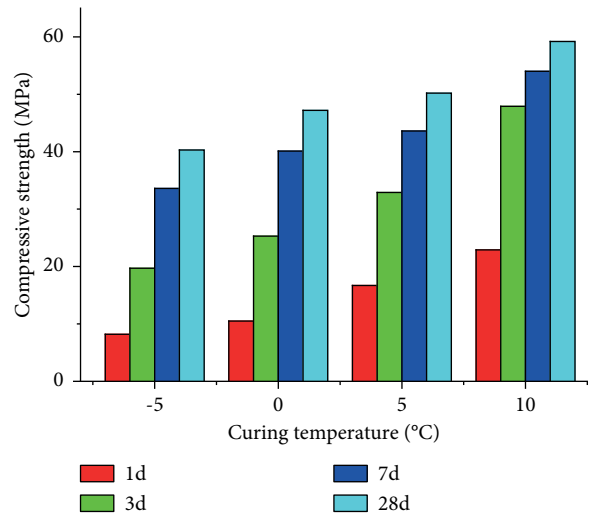

Figure 4: Compressive strength of CSA/GFRC at −5, 0, 5, and 20°C.

3.4. Freeze-Thaw Performance. The compressive strength of CSA/GFRC under freeze-thaw attack is present in Figure 6. It can be found out that with increasing freeze-thaw cycles, compressive strength of CSA/GFRC indicates gradual reduction and this strength reduction is more evident with lower curing temperatures. Beneficial freeze-thaw resistance property can be observed in CSA/GFRC, and the corresponding strength remains 95.9%, 94.7%, 94.2%, and 94.3%, respectively, for that cured under 20°C, 5°C, 0°C, and −5°C after 50 freeze-thaw cycles. This is in consistence with the previous research [18, 19], suggesting that reduction in both flexural strength and dynamic modulus of elasticity of CSA cement mortar is less than 5% after more than 30 cycles of freeze-thaw. The favorable freeze-thaw resistance of CSA/GFRC provides great confidence in its application under low temperatures.

3.5. Microstructure at Interfilamental Space. Microstructure of CSA/GFRC cured at −5°C for 28 d is present in Figure 7. It can be seen from Figure 7(a) that the interfilamentary spaces are partly occupied by hydration products, with some empty voids between fibres occasionally. This densification at the interfilamentary space may result in loss on flexibility when forces are applied [22, 23], which subsequently reduce the post-peak toughness of CSA/GFRC to some extent. This is in agreement with the previous studies concluding that partial densification of the space between fibres by hydrated products may become a deciding microstructural factor in the degradation of GFRC [3, 13, 14]. Elemental mappings were also obtained in this study to investigate the spatial distributions of Ca, S, and Al as shown in Figure 7(b). It can be concluded that elements of Ca, Si, and S are accumulated in the interfilamentary spaces.

In order to investigate the chemical compositions of the hydration phases, spot analysis on three representative points located between fibres is listed in Figure 7(c). The spot analysis results on Point 1 showed a medium accumulation of Ca and S at the interfilamentary zone, involving 26.1 wt. % Ca and 10.0

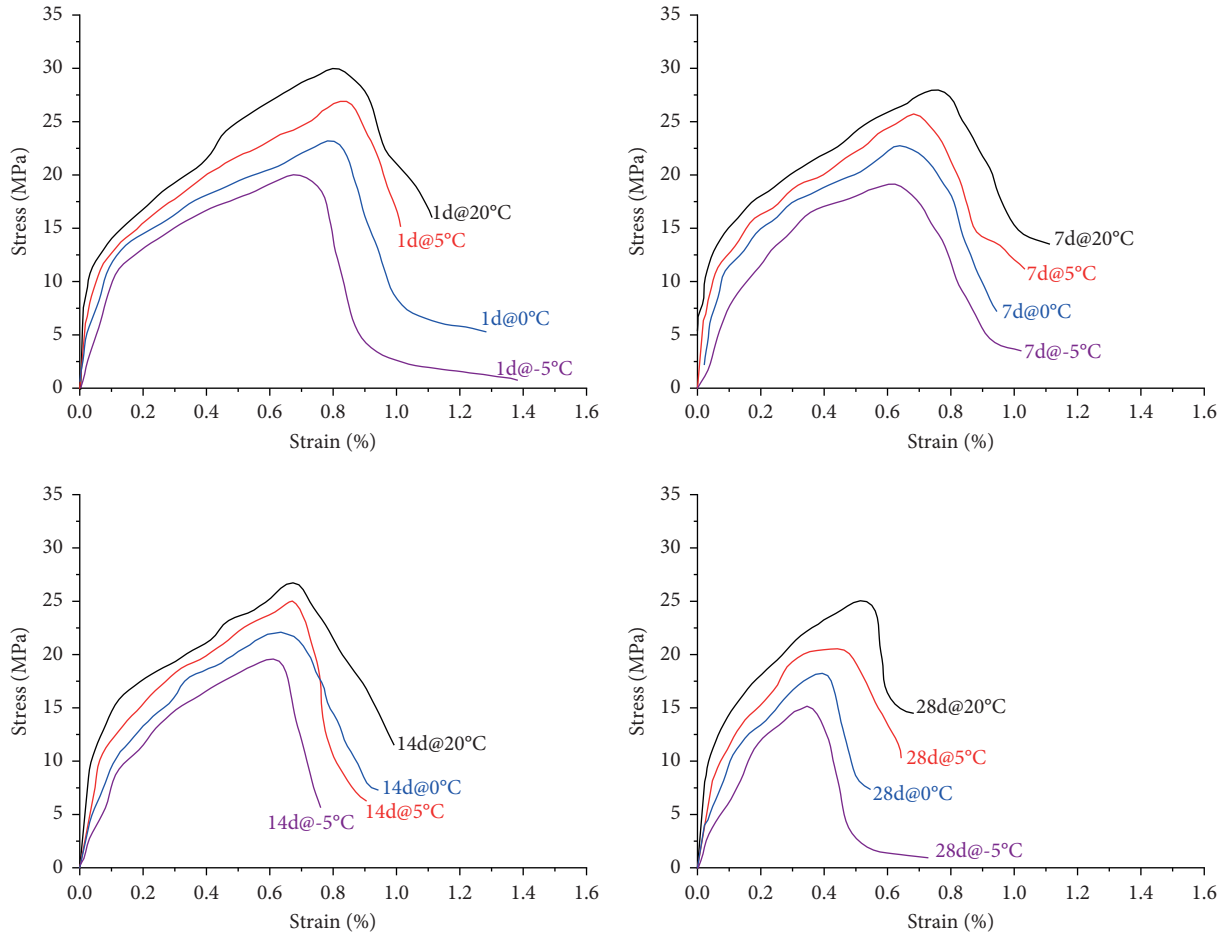

Figure 5: Stress-strain curves of CSA/GFRC at −5, 0, 5, and 20°C at different ages.

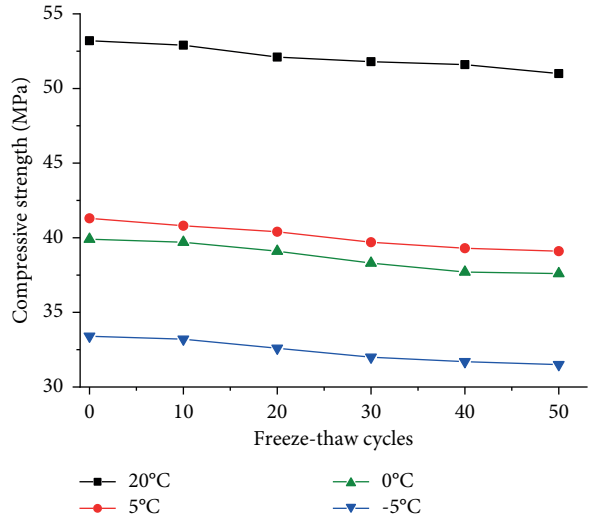

Figure 6: Compressive strength after freeze-thaw cycles.

wt. % S, with small amounts of Al and Si included as well. The corresponding Al/Ca was 0.36 and S/Ca ratio was 0.48 at Point 1, which is considered as ettringite-type phases (Al/Ca = 0.33, S/Ca = 0.5) with small inclusions of C-A-S-H gel. The Al/Ca of Point 2 and 3 reaches 0.54 and 0.55, respectively, with corresponding S/Ca of 0.17 and 0.14. This suggests an increased level of Al inclusion and reduced level of S compared with Point 1. It can be presumed that the main hydration phases at the two points are ettringite intermixed with larger amount of C-A-S-H. Therefore, it can be concluded that hydrated phases

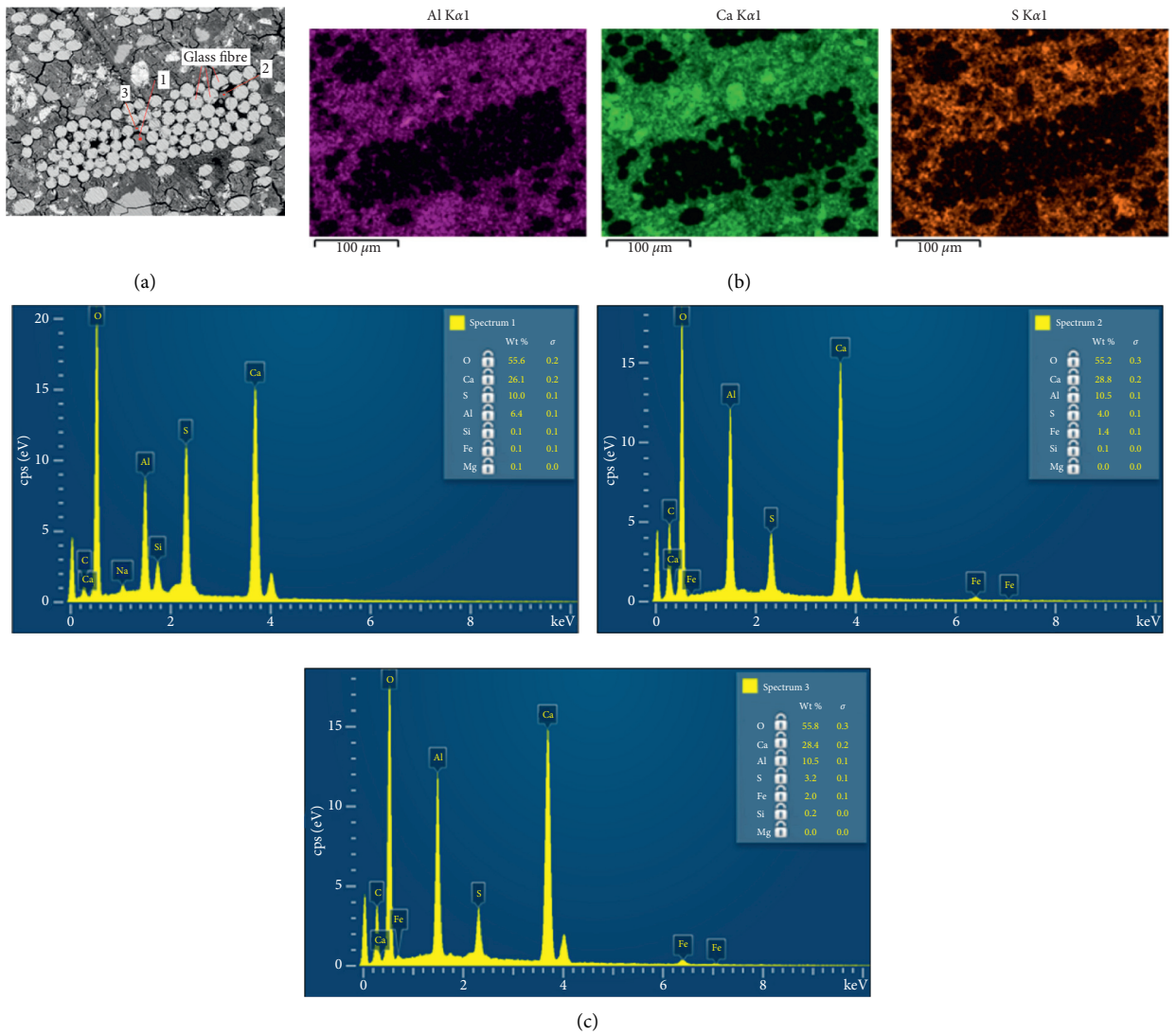

Figure 7: Microstructure of CSA/GFRC cured at −5°C for 28 d: (a) microstructure at interfilamentary spaces; (b) elemental mappings of Ca, Al, and S in CSA/GFRC; (c) EDX result on Point 1, 2, and 3 at the interfilamentary space.

at the interfilamentary space of CSA/GFRC cured under low temperature are mainly ettringite phases finely intermixed with C-A-S-H gels at varying proportions.

4. Conclusions

It can be concluded that low-temperature environment has very little effect on the type of hydration products in hydrated CSA cement. The main hydration product of hydrated CSA cement cured under low temperatures is ettringite which suggests that hydration of CSA cement still continues under lower temperatures.

It can also be found out that low-curing temperatures have an adverse effect on the strength development of CSA/GFRC, but the strength difference compared with that under 20°C reduces gradually with increasing curing ages. Corresponding compressive strength is 40.3 MPa, 47.2 MPa, and 50.2 MPa under −5°C, 0°C, and 5°C for 28 d, which occupies 67.7%, 79.3%, and 84.4% of that under 20°C.

In terms of bending performance, there are insignificant changes in ultimate strain value at low temperatures at early ages, however, but both ultimate tensile strength and ultimate strain value indicate considerable degradation with ageing under low temperatures after 14 d. The ultimate strain value reduces to 0.34% at −5°C, 0.39% at 0°C, and 0.44% at 5°C compared with 0.51% for that cured at 20°C for 28 d. The tensile strength of samples cured at −5°C for 28°d is only 15.2 MPa, taking up only 40% of that under 20°C.

CSA/GFRC also demonstrated great capability in the antifreeze-thaw performance. The corresponding strength remains 95.9%, 94.7%, 94.2%, and 94.3%, respectively, for that cured under 20°C, 5°C, 0°C, and −5°C after 50 freeze-thaw cycles.

Microstructural studies suggest that the interfilamentary spaces are partly occupied by hydration products, with some empty voids between fibres occasionally. Spot analysis on three representative points at the interfilamentary space demonstrates that hydrated phases at the interfilamentary

space of CSA/GFRC cured under low temperature are mainly ettringite phases finely intermixed with C-A-S-H gels at varying proportions. This densification may result in loss on flexibility when forces are applied, therefore reducing the post-peak toughness to some extent. Therefore, studies on how to optimize the interfilamentary spaces with more flexibility are necessary before durable CSA/GFRC can be created and applied in field under low temperatures.

Data Availability

The data used to support the findings of this study are available from the corresponding author upon request.

Conflicts of Interest

The authors declare that there are no conflicts of interest.

Acknowledgments

This project was funded by the National Natural Science Foundation of China (No. 51674199), Key Laboratory of Structure and Wind Tunnel of Guangdong Higher Education Institutes Open Fund (No. 202002), and Natural Science Basic Research Program of Shaanxi Province (No. 2021JQ-605).

References

[1] J. G. Ferreira and F. A. Branco, "Structural application of GRC in telecommunication towers," *Construction and Building Materials*, vol. 21, no. 1, pp. 19–28, 2007.

[2] A. Enfedaque, L. S. Paradela, and V. Sánchez-Gálvez, "An alternative methodology to predict aging effects on the mechanical properties of glass fiber reinforced cements (GRC)," *Construction and Building Materials*, vol. 27, no. 1, pp. 425–431, 2012.

[3] M. Butler, V. Mechtcherine, and S. Hempel, "Durability of textile reinforced concrete made with AR glass fibre: effect of the matrix composition," *Materials and Structures*, vol. 43, no. 10, pp. 1351–1368, 2010.

[4] A. Enfedaque, D. Cendón, F. Gálvez, and V. Sánchez-Gálvez, "Failure and impact behavior of facade panels made of glass fiber reinforced cement (GRC)," *Engineering Failure Analysis*, vol. 18, no. 7, pp. 1652–1663, 2011.

[5] P. Purnell and J. Beddows, "Durability and simulated ageing of new matrix glass fibre reinforced concrete," *Cement and Concrete Composites*, vol. 27, no. 9-10, pp. 875–884, 2005.

[6] A. Nourredine, "Influence of curing conditions on durability of alkali-resistant glass fibres in cement matrix," *Bulletin of Materials Science*, vol. 34, no. 4, pp. 775–783, 2011.

[7] M. A. Boumehraz, M. Mellas, K. Goudjil, and F. Boucetta, "Study of the aging of a concrete reinforced by alkali resistant glass fiber in the wet environment," *Annales de Chimie Science des Matériaux*, vol. 44, no. 2, pp. 85–90, 2020.

[8] J. S. Damtoft, J. Lukasik, D. Herfort, D. Sorrentino, and E. M. Gartner, "Sustainable development and climate change initiatives," *Cement and Concrete Research*, vol. 38, no. 2, pp. 115–127, 2008.

[9] F. P. Glasser and L. Zhang, "High-performance cement matrices based on calcium sulfoaluminate–belite compositions," *Cement and Concrete Research*, vol. 31, no. 12, pp. 1881–1886, 2001.

[10] C. Hu, D. Hou, and Z. Li, "Micro-mechanical properties of calcium sulfoaluminate cement and the correlation with microstructures," *Cement and Concrete Composites*, vol. 80, pp. 10–16, 2017.

[11] L. H. J. Martin, F. Winnefeld, E. Tschopp, C. J. Müller, and B. Lothenbach, "Influence of fly ash on the hydration of calcium sulfoaluminate cement," *Cement and Concrete Research*, vol. 95, pp. 152–163, 2017.

[12] T. Lee, J. Lee, and H. Choi, "Effects of accelerators and retarders in early strength development of concrete based on low-temperature-cured ordinary Portland and calcium sulfoaluminate cement blends," *Journal of Materials*, vol. 13, no. 7, p. 1505, 2020.

[13] R. Trauchessec, J. M. Mechling, A. Lecomte, A. Roux, and L. Rolland, "Hydration of ordinary Portland cement and calcium sulfoaluminate cement blends," *Cement and Concrete Composites*, vol. 56, pp. 106–114, 2015.

[14] M. Borstnar, N. Daneu, and S. Dolenec, "Phase development and hydration kinetics of belite-calcium sulfoaluminate cements at different curing temperatures," *Ceramics International*, vol. 46, no. 18, pp. 29421–29428, 2020.

[15] M. Song, P. Purnell, and I. Richardson, "Microstructure of interface between fibre and matrix in 10-year aged GRC modified by calcium sulfoaluminate cement," *Cement and Concrete Research*, vol. 76, pp. 20–26, 2015.

[16] M. Song, K. Wu, and Y. Dou, "Durability of GFRC modified by calcium sulfoaluminate cement under elevated curing temperatures," *Advances in Materials Science and Engineering*, vol. 2019, Article ID 2915684, 6 pages, 2019.

[17] J. Péra and J. Ambroise, "New applications of calcium sulfoaluminate cement," *Cement and Concrete Research*, vol. 34, no. 4, pp. 671–676, 2004.

[18] L. Li, R. Wang, and Q. Lu, "Influence of polymer latex on the setting time, mechanical properties and durability of calcium sulfoaluminate cement mortar," *Construction and Building Materials*, vol. 169, pp. 911–922, 2018.

[19] I. Janotka and L. È Krajèi, "Resistance to freezing and thawing of mortar specimens made from sulphoaluminate-belite cement," *Bulletin of Materials Science*, vol. 23, no. 6, pp. 521–527, 2000.

[20] Q. Huang, X. Zhu, D. Liu, L. Zhao, and M. Zhao, "Modification of water absorption and pore structure of high-volume fly ash cement pastes by incorporating nanosilica," *Journal of Building Engineering*, vol. 33, no. 3, Article ID 101638, 2020.

[21] X. Zhu, M. Zhang, Y. Yang, K. Yang, and F. Wu, Q. Li, L. Yu, C. Yang, and M. Basheer, "Understanding the aqueous phase of alkali-activated slag paste under bath-curing," *Advances in Cement Research*, vol. 33, no. 2, pp. 1–33, 2019.

[22] J. Gong, Z. Li, R. Zhang, J. Li, and X. Shi, "Synergistic effects of nano-montmorillonite and polyethylene microfiber in foamed paste with high volume fly ash binder," *Journal of Nanoscience and Nanotechnology*, vol. 19, pp. 4465–4473, 2019.

[23] Z. Li, J. Gong, S. Du et al., "Nano-montmorillonite modified foamed paste with a high volume fly ash binder," *RSC Advances*, vol. 7, p. 9803, 2017.